

Localization of light in subradiant Dicke states

Giuseppe Luca Celardo

Dipartimento di Matematica e Fisica and ILAMP, Università Cattolica del Sacro Cuore, Brescia, ITALY
Istituto Nazionale di Fisica Nucleare, sez. Pavia, Pavia, ITALY and
Benemérita Universidad Autónoma de Puebla, Instituto de Física, Apartado Postal J-48, Puebla 72570, Mexico

Mattia Angeli

Dipartimento di Matematica e Fisica and ILAMP, Università Cattolica del Sacro Cuore, Brescia, ITALY

R. Kaiser

Université Côte d'Azur, CNRS, Institut de Physique de Nice, Valbonne F-06560, France
 (Dated: February 16, 2017)

Anderson localization of light in three dimensions has challenged experimental and theoretical research for the last decades. Here we propose a novel route towards this goal accessible in a dilute sample of cold atoms. We show that disorder in atomic transition frequencies can result in localization of light in subradiant Dicke states. The effective Hamiltonian of the coupled dipole model allowed us to exhibit strong signature of a transition to localization of subradiant states and we show that the critical disorder required for this transition scales as the product of the on-resonant optical depth of the samples times the lifetime of the subradiant states. This scaling also allows to define a critical lifetime, above which the states are localized.

PACS numbers:

Strong localization, i.e. the absence of diffusion in a disordered sample, is an interference phenomenon proposed by Anderson in 1958 to explain the transition between a metallic and an insulating phase [1]. Coherent transport continues to pose many questions at a fundamental level. Whereas the beauty of the Anderson model lies in its underlying simplicity and assumed universality, it is fundamental to verify its predictions in realistic systems. In particular we have to understand to what extent microscopic details can affect the consequences of interferences in disordered systems. Although for electrons in solids interactions prominently affect their transport properties, even the simpler case of non-interacting wave propagation in disordered systems still challenges our understanding of strong localization. It is therefore essential to investigate a variety of systems with different properties to look for universal features. Interferences in disordered systems have thus been at the focus of an ever increasing research community, ranging from condensed matter to acoustics, optics and ultracold matter waves [2–11]. Light has been an obvious candidate to study Anderson localization of non-interacting waves, which has triggered continuous efforts since the mid-80s [12–22]. The assumed universality of Anderson localization of non-interacting waves seemed to be confirmed by a variety of experiments. Anderson localization of light in three dimensions however challenges this common believe. It has now been shown that past experiments on Anderson localization of light [15–17] do not provide a signature for the Anderson transition in three dimensions [18–22]. Moreover, even though details at the microscopic level had not been expected to be essential, the mere existence of an Anderson phase transition for light is now being questioned. Indeed, initial conjectures and experimental efforts for Anderson localization of light in three dimensions did not take into account the polarization of the photons and the associated near-field coupling between scatterers. They also neglected the fact that the in-

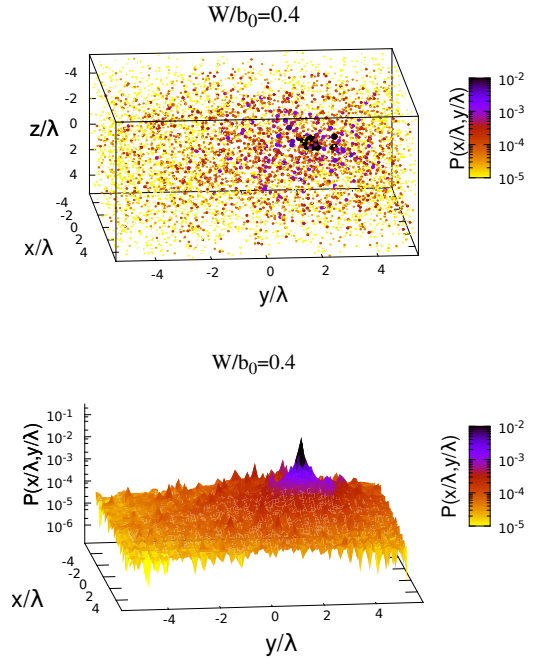


FIG. 1: (Color online) Representations of a typical subradiant localized state. Here is $N = 6400$, $\rho\lambda^3 = 5$ corresponding to $b_0 \approx 17.3$ and $W/b_0 = 0.4$. For the state shown here, we have $\Gamma = 0.094$, $E = 0.1$ and a participation ratio $PR \approx 7$. In the upper panel each atom is shown by a small sphere with a radius increasing with the probability $|\Psi_j(r)|^2$ for the excitation to be located on that atom. Also the color depends on $|\Psi_j(r)|^2$. In the lower panels the projection on the $x - y$ plane of $|\Psi_j(r)|^2$ on a grid of 60×60 is shown. More details about the two panels can be found in Supp. Mat., together with the representation of a typical extended state.

interactions induced between the atoms by the electromagnetic field have a long range nature, which is thought to destroy localization [23–25]. Moreover, the outgoing scattering component of the electromagnetic wave makes the situation of Anderson localization of light an open quantum (wave) problem, where cooperative effects [26–29] significantly change the behaviour, a feature not taken into account in the standard approach of Anderson localization of waves.

Shortly after the publication of the role of the near field dipole-dipole coupling on the existence of Anderson localization in dense samples of cold atoms [30, 31], alternative routes towards Anderson localization of light by cold atoms have been investigated. One approach consists of applying a strong magnetic bias field, which in effect decouples some of the excited magnetic sublevels of the atoms [32]. Here we propose another approach, based on the existence of subradiant Dicke states [28, 33, 34]. In the dilute limit and a system size much larger than the wavelength, we will show that these states can be localized by additional diagonal disorder on top of positional disorder of the atoms, which can be understood as the equivalent of off-diagonal disorder in an Anderson model. In the case of cold atoms, diagonal disorder corresponds to random shifts of the transition frequencies.

Here we consider a realistic model of dipole-dipole coupling [35] well suited to describe coherent multiple scattering of light in a sample of two-level systems. Following the previous discussion and previous results in Ref. [36–38], we investigate the possibility of localization to occur in the subradiant subspace, where shielding from long range hopping should be effective [39, 40], thus allowing for localization to occur [39]. Indeed in Ref. [36, 37], where a 1D and 3D Anderson lattice model coupled to a common decay channel was considered, the system response to diagonal disorder has been shown to be strongly dependent on the life time of its eigenmodes. Specifically, due to the diagonal disorder, subradiant states become hybrid states with both an exponentially localized component corresponding the Anderson localized state of the closed system and a superimposed extended background, induced by the residual long range hopping.

This paper is organized as follows: first we present the model and the tools exploited to exhibit the signatures of localization of light in subradiant Dicke states. We then present our numerical results and discuss the scaling laws for the required diagonal disorder to be able to induce localization of subradiant states.

The Model.— We consider a 3D cloud of N atoms randomly distributed inside a cube of volume $V = L^3$. Introducing the density $\rho = N/L^3$ and the wavevector $k = 2\pi/\lambda$ we define the mean free path $l = 1/\rho\sigma$, where $\sigma = 4\pi/k^2$ is the scattering cross section. Finally, we define the optical thickness, b_0 , as the ratio between the system size L and the mean free path l :

$$b_0 = \frac{L}{l} = \rho \frac{4\pi}{k^2} \left(\frac{N}{\rho}\right)^{1/3}. \quad (1)$$

The optical thickness can be also related to the number of atoms which compete to decay in the same electromagnetic

channel and can thus be understood as a measure of the cooperativity of the system [26, 31, 41]. Indeed since the number M of electromagnetic channels $M \propto (L/\lambda)^2$, we can write $b_0 \propto N\lambda^2/L^2 \propto N/M$.

We considered the single excitation effective Hamiltonian in the scalar approximation [35]. This approximation is appropriate in the dilute limit, where interatomic distances are larger than the optical wavelength, making near field terms decaying as $1/r^3$ negligible. As we will see, and in contrast to common believe that high spatial densities (with a correspondingly very short scattering mean free path for the photons) are required for localization, we will exhibit localization of light in such a dilute limit.

The effective Hamiltonian which governs the interaction of the atoms with the electromagnetic field in this limit is characterized by long range hopping terms $V_{i,j}$ decreasing as $1/r_{ij}$ with the distance:

$$\mathcal{H} = \sum_{i=1}^N (E_i - i\frac{\Gamma_0}{2}) |i\rangle \langle i| + \frac{\Gamma_0}{2} \sum_{i \neq j}^N V_{i,j} |i\rangle \langle j| \quad (2)$$

where the state $|i\rangle$ stand for the i -atom in the excited state and all the other atoms being in the ground state, $V_{i,j} = \frac{\exp(ik_0 \cdot r_{ij})}{k_0 \cdot r_{ij}}$ is the interaction between the atoms at distance r_{ij} . Γ_0 is the natural decay width for a single atom. In the following energies and decay widths of the states will be expressed in units of Γ_0 . Note that \mathcal{H} contains both real and imaginary parts which takes into account that the excitation is not conserved since it can leave the system by emission. This situation is thus reminiscent of an open quantum (wave) system.

The complex eigenvalues of this Hamiltonian describe the energy and linewidths of the eigenmodes of the system. We stress that even in the dilute limit $\rho\lambda^3 \ll 1$ we can have cooperative behaviour in the large sample limit ($L \gg \lambda$), provided that the cooperativity parameter $b_0 \gg 1$. In this regime cooperative effects such as single excitation sub- and superradiance become relevant [28, 33, 34]. Superradiant states are characterized by a decay width which is larger than the single atom natural width Γ_0 , while subradiant states have a decay widths which are much smaller than the single atom decay width, as experimentally observed in dilute clouds of cold atoms [33].

In addition to the positional disorder of the atoms as studied previously [30, 31], we now introduce an additional random diagonal disorder term in the Hamiltonian, E_i , which shifts the excitation energy of the atoms. Experimentally in cold atomic clouds, such on-site disorder can be realized by applying a speckle field coupling the excited state to an auxiliary other excited state with convenient detuning, inducing thus random shifts of the atomic resonances without inducing dipole forces in the ground state. Following the approach of the Anderson model on lattice, we allow the site energies to fluctuate in the range of $[-W/2, +W/2]$, where W is the strength of disorder (in units of Γ_0). Ensemble averaging thus includes different realizations of the random position of the atoms and of the random disorder strengths.

Within this model, we can now study different regimes using a variety of indicators to illustrate the rich phenomena in-

cluded in this Hamiltonian. First, we can study the eigenvalues as has been done in [30, 31] and the spatial profile of the eigenstates, which provide striking evidence when spatially localized eigenstates emerge [42]. In a more quantitative way, we also studied the participation ratio [43, 44],

$$PR = \left\langle 1 / \sum_i |\langle i | \psi \rangle|^4 \right\rangle, \quad (3)$$

of the eigenstates $|\psi\rangle$ of the Hamiltonian Eq.(2), where $\langle \dots \rangle$ stands for the ensemble average over different realizations of the static disorder and positional disorder. This participation ratio is a very convenient indicator of localization, as for extended states, it increases proportionally to the system size, N , while, for localized states, it is independent of N .

Note that, since the atoms are randomly placed in a fixed volume, there will be a certain probability of two atoms being located very close to each other. This will induce pair-physics effects which should be neglected since here we are looking for collective effects (localization over many atomic states). We have avoided such pair-physics by a proper selection of the interval of complex energies as it has been done in previous works [30, 31]. Alternatively these effects can also be avoided by including an exclusion volume around each atom [33, 34].

Localization Transition: critical disorder.— A very striking illustration of the existence of localized states described by our Hamiltonian is given in Fig. 1, where we represent a typical localized subradiant eigenstate for $N = 6400$, $\rho\lambda^3 = 5$ so that $b_0 \approx 17.3$ and with a disorder of $W/b_0 = 0.4$. The eigenstate belongs to the energy window $-0.1 < E < 0.25$ (the real part of the eigenvalues) and resonance widths window of $0.046 < \Gamma < 0.1$ (the imaginary part of the eigenvalues). The upper panel shows a 3D representation of the eigenstates, while the lower panels show the projection of $|\psi(r)|^2$ on the $x - y$ plane, see Supp. Mat. for more details. The addition of sufficient diagonal disorder, on top of the positional disorder, allows to obtain localized states, even in the dilute limit, where the Ioffe-Regel criterion (in absence of diagonal disorder) for localization ($kl = 2\pi^2/\rho\lambda^3 \approx 4 > 1$) is not fulfilled. We observe that the localized peak, shown in Fig. (1 lower panel), come hand in hand with an extended tail. This is consistent with what was found in Ref [36, 37], where it was shown that the nature of the subradiant localized states is hybrid, with a central localized component reminiscent of an Anderson localized state in absence of opening to outgoing channels and a plateau reminiscent of residual extended subradiant component.

In order to study the localization transition, we performed a systematic analysis of the participation ratio *vs* the disorder strength W for different densities, system sizes and window of decay widths. A typical example of our analysis is shown in Fig. 2, where we analyze the localization properties of the eigenmodes of the system for different system size at fixed density $\rho\lambda^3 = 5$ and two different windows of decay widths: a group of subradiant states ($0.046 < \Gamma < 0.01$) is shown in the left panels, while a group of superradiant states ($1 < \Gamma < 2.15$) is shown in the right panels. A clear signature of a transition to localization can be seen for the subradi-

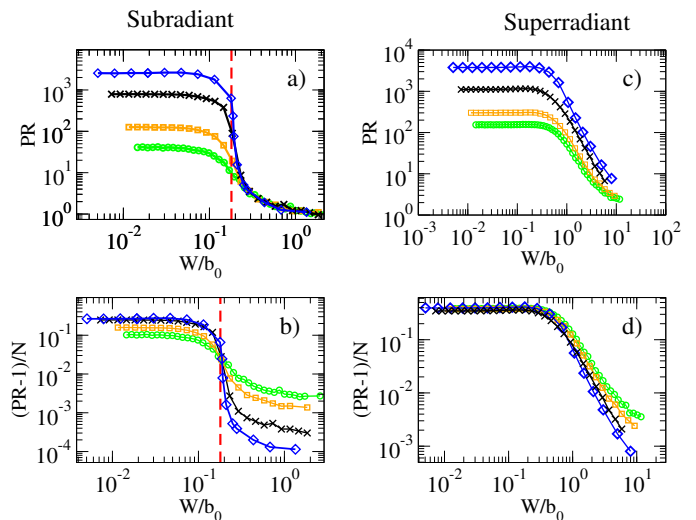


FIG. 2: (Color online) Average participation ratio Eq.(3) for subradiant states (left panels) and superradiant states (right panels) as a function of the rescaled disorder W/b_0 and different system sizes as indicated below. Above a critical disorder indicated by the red vertical dashed line, the participation ratio of the subradiant states become independent of N (upper left panel), whereas the participation ratio of superradiant states keep increasing with N (upper right panel). The normalized participation ratio shows the critical disorder separating the extended from the localized regime for the subradiant states (lower left panel), whereas no clear transition occurs for the superradiant states (lower right panel). The average was done over disorder and different eigenvalues in the interval $-0.1 < E < 0.25$ (the real part of the eigenvalue). The interval of widths is $0.046 < \Gamma < 0.1$ for the subradiant states (left panels) and $1 < \Gamma < 2.15$ for the superradiant states. The density is $\rho\lambda^3 = 5$ in all panels. Note that for each N we have different values of $b_0 = 6.8$ ($N = 400$, green circles), 8.6 ($N = 800$, orange squares), 13.7 ($N = 3200$, black crosses), 19.8 ($N = 9600$, blue rombs).

ant states when the disorder strength is rescaled by the optical thickness b_0 . In Fig. 2(a), we show that below a critical W/b_0 indicated by the vertical dashed line, the participation ratio of the selected subradiant states increase with the atom number, an indication of extended states. Above the critical W/b_0 however, the participation ratio becomes independent of the atom number, as expected from localized states. A more precise study of the transition point can be obtained when looking at the normalized participation ratio as shown in Fig. 2(b) for the subradiant states: a universal crossing occurs which allows to determine the value of the critical W/b_0 for the localization transition. Even if a weak crossing can be observed also for the superradiant states when looking at the normalized participation ratio (Fig. 2(d)), their behaviour is in striking contrast to the behaviour of the subradiant states. Indeed the PR of the superradiant states is affected by disorder at much larger values of W/b_0 and, most importantly, it does not become independent of the system size for any disorder considered, see Fig. 2(c). We have verified that our analysis of the participation ratio also captures the localization transition studied in [30, 31], see Supp. Mat.

By performing a similar analysis as in Fig. 2(b), for differ-

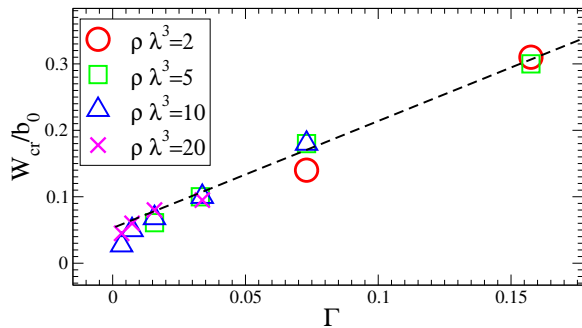


FIG. 3: (Color online) Critical disorder for localization: W_{cr} rescaled by b_0 is plotted vs the mean Γ for different densities, see figure. The black dashed line shows a fit given in Eq. (4).

ent densities and window of decay width, we determined the dependence of the critical disorder on b_0 , Γ and ρ . We focused our analysis to the subradiant states, where a clear transition to localization has been observed. The result is illustrated in Fig. 3, where a linear dependence of W_{cr}/b_0 vs Γ is clearly shown for sufficiently large values of Γ . The result can be summarized in the fitting formula of the critical disorder given by:

$$W_{cr} \sim 1.61b_0\Gamma + 0.053b_0, \quad (4)$$

where both W_{cr} and Γ are in units of Γ_0 . We also note that for high spatial densities and very small Γ a deviation from this law is observed, which lowers the values of the critical disorder needed to have a transition to localization.

Localization Transition: critical decay width.— The critical disorder Eq. (4) depends not only on b_0 but also on the decay width of the subradiant states considered. Interestingly, from Eq. (4) one can determine the critical decay width for fixed b_0 , N , ρ , W below which we have localized states. Indeed from Eq. (4) we can write $\Gamma_{cr} \approx (W/b_0 - 0.053)/1.61$, so that the critical decay width below which subradiant states are localized, increases with the normalized disorder W/b_0 . To further study the relationship between lifetime and localization, we now turn to the eigenvalues of the Hamiltonian and the participation ratio of each eigenstate, see Fig.(4 upper panel). For all values of the energy E , a sharp transition in the participation ratio is visible for a given value of Γ . This transition line (obtained from Eq. (4)), indicated by the dashed horizontal line in Fig. 4 upper panel, corresponds to the appearance of a localized component on top a flat background. The appearance of a critical decay width is a novel feature of the transition to localization in open quantum wave systems in presence of cooperativity (sub- and superradiance). Interestingly it points to the existence of a “mobility edge” in the imaginary axis. Indeed, as shown in Fig. 4 lower panel, the PR of the subradiant states is independent of the system size below Γ_{cr} (see vertical dashed line) if W/b_0 is kept fixed. Even though the present results are in line with the initial toy model of Ref. [36, 37], there the dependence on the lifetime of the subradiant eigenmodes was not apparent. Indeed, in that open 3D Anderson model the sub- and superradiant modes were segregated in two regions and only their global

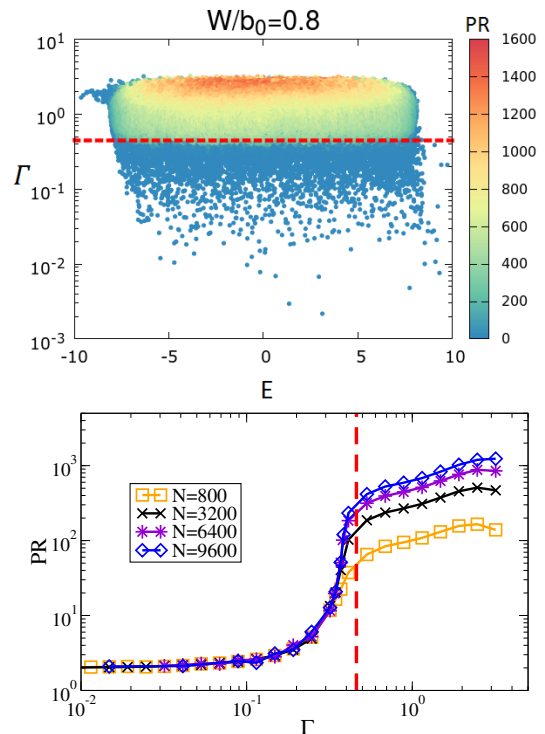


FIG. 4: (Color online) Upper panel: Participation ratio of the eigenstates in the complex plane E, Γ (in units of Γ_0) of the eigenvalues of each state. Here $N = 9600$, $\rho\lambda^3 = 5$, $b_0 \approx 19.8$ and $W/b_0 = 0.8$. The scale of the participation ratio is given in the color code. The critical width of the resonance for the transition to localization (obtained inverting Eq.(4)) is indicated by the red horizontal line. Lower Panel: Average participation ratio as a function of the decay width of the eigenstates. Here the normalized disorder is kept fixed at $W/b_0 = 0.8$. The density is $\rho=5$ and we have considered the eigenstates in the range $-0.1 < E < 0.25$. Note that for each N we have different values of $b_0 = 8.6$ ($N = 800$, orange squares), 13.7 ($N = 3200$, black crosses), 17.3 ($N = 6400$, violet stars), 19.8 ($N = 9600$, blue rombs). Two different regimes can be seen: one in which the PR is independent of N (for low values of Γ) and one where the PR depends on N (for large values of Γ). The red dashed line indicate the critical width obtained inverting Eq. (4).

behaviour were analyzed. In the present case, no gap between sub- and superradiant modes exists.

Conclusions.— In conclusion, we have analyzed the localization properties of light by a three dimensional atomic cloud. We have shown that localization of light is possible even when the cloud is dilute, i.e. in a regime where, in the absence of diagonal disorder, the scattering mean free path of photons remains larger than the optical wavelength. In presence of strong cooperativity (super- and subradiance), localization is achieved in the subradiant subspace by introducing random spatial fluctuations of the transition frequency of the atoms. The critical disorder which we determined for the transition to the localization depends linearly on the optical thickness and the average decay width of the states considered. Our results can pave the way to experimentally realize localization of light in dilute three dimensional atomic clouds. This is thus

an alternative route [32] to avoid near field dipole-dipole coupling which is expected to prevent localization for high spatial densities [30, 31].

W. Guerin.

Acknowledgments

We acknowledge stimulating discussions with R. Bachelard, A. Biella, F. Borgonovi, G. G. Giusteri and

-
- [1] P. W. Anderson, *Phys. Rev.* **109**, 1492 (1958).
 [2] P. A. Lee and T. V. Ramakrishnan, *Rev. Mod. Phys.* **57**, 287 (1985).
 [3] A. Lagendijk, B. A. van Tiggelen, *Phys. Rep.* **270**, 143 (1996).
 [4] E. Akkermans and G. Montambaux, *Mesoscopic physics of electrons and photons*, Cambridge Univ. Press (2007).
 [5] A. Lagendijk, B. van Tiggelen, D. S. Wiersma, *Phys. Today* **62**, 24 (2009).
 [6] A. Aspect, M. Inguscio, *Phys. Today* **62**, 30 (2009).
 [7] H. Hu, A. Strybulevych, J.H. Page, S.E. Skipetrov, B.A. van Tiggelen, *Nature Phys.* **4**, 945 (2008).
 [8] J. Chabé et al., *Phys. Rev. Lett.* **101**, 255702 (2008).
 [9] S. S. Kondov, W. R. McGehee, J. J. Zirber, B. DeMarco, *Science* **334**, 66 (2011).
 [10] F. Jendrzejewski et al., *Nature Phys.* **8**, 398 (2012).
 [11] G. Semeghini et al., *Nature Phys.* **11**, 554 (2015).
 [12] S. John, *Phys. Rev. Lett.* **53**, 2169 (1984).
 [13] S. John, *Phys. Rev. Lett.* **58**, 2486 (1986).
 [14] P. W. Anderson, *Philos. Mag. B* **52**, 505 (1985).
 [15] D. S. Wiersma, P. Bartolini, A. Lagendijk, R. Righini, *Nature* **390**, 671 (1997).
 [16] C. M. Aegerter, M. Störzer, G. Maret, *Europhys. Lett.* **75**, 562 (2006).
 [17] T. Sperling, W. Bührer, C.M. Aegerter, G. Maret, *Nature Photon.* **7**, 48 (2013).
 [18] F. Scheffold, R. Lenke, R. Tweer, G. Maret, *Nature* **398**, 206 (1999).
 [19] T. van der Beek, P. Barthelemy, P. M. Johnson, D. S. Wiersma, A. Lagendijk, *Phys. Rev. B* **85**, 115401 (2012).
 [20] F. Scheffold, D. Wiersma, *Nature Photon.* **7**, 934 (2013).
 [21] T. Sperling et al., *New. J. Phys.* **18**, 013039 (2016).
 [22] S. E. Skipetrov, J. H. Page, *New. J. Phys.* **18**, 021001 (2016).
 [23] L.S. Levitov, *Europhys. Lett.* **9**, 83 (1989).
 [24] L.S. Levitov, *Phys. Rev. Lett.* **64**, 547 (1990).
 [25] F. Evers and A.D. Mirlin, *Rev. Mod. Phys.* **80**, 1355 (2008).
 [26] E. Akkermans, A. Gero, and R. Kaiser, *Phys. Rev. Lett.* **101**, 103602 (2008).
 [27] R. Kaiser, *J. Mod. Opt.* **56**, 2082 (2009).
 [28] T. Bienaime, N. Piovella, and R. Kaiser, *Phys. Rev. Lett.* **108**, 123602 (2012).
 [29] E. Akkermans and A. Gero, *Euro Phys. Lett.* **101**, 54003 (2013).
 [30] S. E. Skipetrov, and I. M. Sokolov, *Phys. Rev. Lett.* **112**, 023905 (2014).
 [31] L. Bellando, A. Gero, E. Akkermans, and R. Kaiser, *Phys. Rev. A* **90**, 063822 (2014).
 [32] S.E. Skipetrov and I.M. Sokolov, *Phys. Rev. Lett.* **114**, 053902 (2015).
 [33] W. Guerin, M. O. Araújo, and R. Kaiser, *Phys. Rev. Lett.* **116**, 083601 (2016).
 [34] M. O. Araújo, I. Kresić, R. Kaiser, and W. Guerin *Phys. Rev. Lett.* **117**, 073002 (2016).
 [35] S. Bux, E. Lucioni, H. Bender, T. Bienaime, K. Lauber, C. Stehle, C. Zimmermann, S. Slama, Ph. W. Courteille, N. Piovella and R. Kaiser, *J. Mod. Opt.* **57**, 2082 (2010).
 [36] G.L. Celardo, A. Biella, L. Kaplan, F. Borgonovi *Fortschr. Phys.* **61**, 250-260 (2013).
 [37] A. Biella, F. Borgonovi, R. Kaiser, G.L. Celardo, *EuroPhys. Lett.* **103**, 57009 (2013).
 [38] G.G. Giusteri, F. Mattiotti and G. L. Celardo, *Phys. Rev. B* **91**, 094301 (2015); G. L. Celardo, Giulio G. Giusteri, and F. Borgonovi, *Phys. Rev. B* **90**, 075113 (2014).
 [39] G. L. Celardo, R. Kaiser, and F. Borgonovi, *Phys. Rev. B* **94**, 144206 (2016).
 [40] L. F. Santos, F. Borgonovi and G. L. Celardo, *Phys. Rev. Lett.* **116**, 250402 (2016).
 [41] W. Guerin, M.-T. Rouabah, R. Kaiser, *J. Mod. Opt.* (2016): <http://dx.doi.org/10.1080/09500340.2016.1215564>.
 [42] C. E. Maximo, N. Piovella, Ph. W. Courteille, R. Kaiser, R. Bachelard, *Phys. Rev. A* **92**, 062702 (2015).
 [43] A Rodriguez, V A Malyshev and F. Dominguez-Adame, *J. Phys. A: Math. Gen.* **33**, L161 (2000).
 [44] A. Rodriguez, V.A. Malyshev, G. Sierra, M.A. Martin-Delgado, J. Rodriguez-Laguna, F. Dominguez-Adame, *Phys. Rev. Lett.* **90**, 027404 (2003).

Supplementary material for EPAPS

Localization of light in subradiant Dicke states

Giuseppe Luca Celardo^{1,2,3}, Mattia Angeli¹, Robin Kaiser⁴

¹Dipartimento di Matematica e Fisica and ILAMP, Università Cattolica del Sacro Cuore, Brescia, ITALY

²Istituto Nazionale di Fisica Nucleare, sez. Pavia, Pavia, ITALY

³Instituto de Física, Benemérita Universidad Autónoma de Puebla, Apartado Postal J-48, Puebla 72570, Mexico

⁴Université Côte d'Azur, CNRS, Institut de Physique de Nice, Valbonne F-06560, France

A. Extended subradiant state

Here we show an example of a typical extended subradiant state in presence of no diagonal disorder $W/b_0 = 0$, see Fig. (5). This figure should be compared with Fig. (1) of the main text where a typical localized subradiant state with $W/b_0 = 0.4$ is shown. Comparing the two figures one can see that disorder in the transition frequencies of the atoms can induce localized states in the subradiant subspace. In both Fig. (5) and Fig. (1) of the main text, in the upper panels each atom is shown by a small sphere. The probability $|\Psi_j(r)|^2$ for the eigenstate to be on that atom is given by the color and the radius R of the sphere according to the relation $R(r) = 1.5(|\Psi_j(r)|^2/|\Psi_j(r)|_{max}^2)^{2/7}$, where $|\Psi_j(r)|_{max}^2$ is the maximal probability for the case $W/b_0 = 0.4$. This normalization relation was chosen to improve visibility. In the lower panels the projection on the $x - y$ plane of $|\Psi_j(r)|^2$ on a grid of 60×60 is shown. To improve the quality of the representation, each grid point has been averaged by the surrounding points, with a weighting inversely proportional to their distances squared.

B. Localization and density

Here we compare our analysis of the localization properties of the scalar model for cold atomic clouds with the results obtained in previous works, which used a resonance overlap or Thouless parameter as indicator for localization [30, 31]. As reported in Ref. [30, 31] the scalar model predicts Anderson localization at high densities in cold atomic clouds (mainly due to the positional disorder) even in the absence of diagonal disorder. In Fig. 6 the mean PR as a function of the density of a group of subradiant states is shown at a fixed disorder (considerably lower than W_{cr}). When the densities are large enough ($\rho\lambda^3 > 24$) these states are indeed localized, above a critical density which is in excellent agreement with Ref. [30, 31]. In order to avoid such a high density transition, we kept the densities analyzed in the main text at values well below that critical value. Note however that at large densities the scalar model is not a good description of atom-light cou-

pling and a more refined models, including polarization and near field dipole-dipole coupling, does not show signatures of localization in the dense limit [30, 31]. On the other side, the

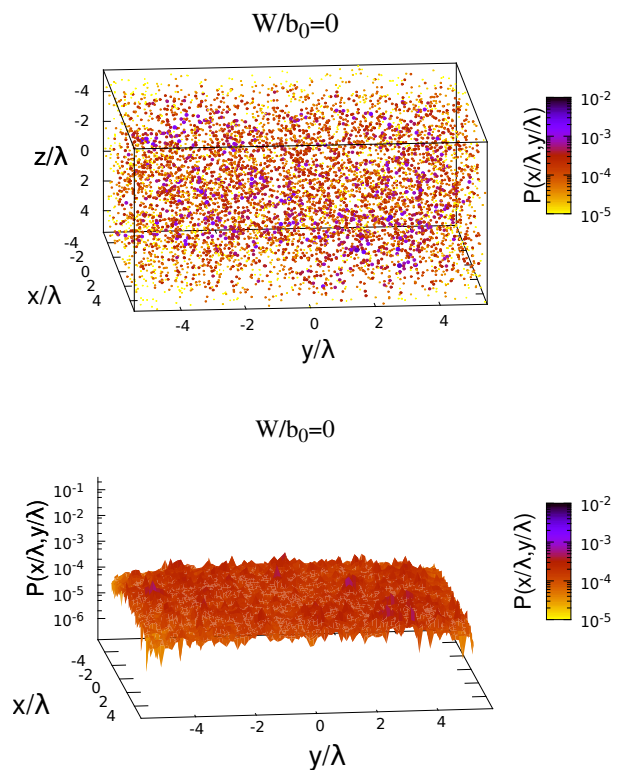


FIG. 5: (Color online) Representations of a typical extended subradiant state. Here is $N = 6400$, $\rho\lambda^3 = 5$ so that $b_0 \approx 17.3$ and $W/b_0 = 0$. For the state shown we have $E = -0.0758$, $\Gamma = 0.05$. The participation ratio PR , defined in Eq. (3), of the state shown in this figure we have $PR = 1941$. Details about the two panels can be found in the text.

localization transition observed in the dilute limit in the main text is experimentally relevant.

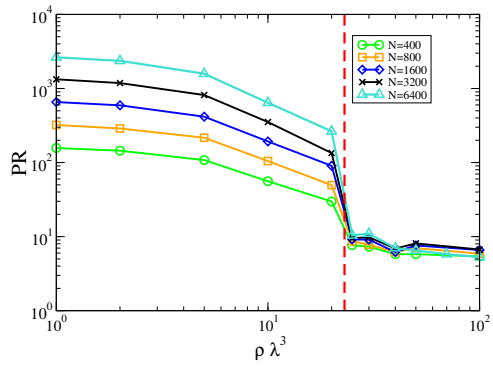


FIG. 6: (Color online) Average participation ratio of a group of sub-radiant states with $0.01 < \Gamma < 1$ as a function of the density $\rho \lambda^3$ at fixed very small disorder $W \approx 0.1$. The transition to localization occur at $\rho \approx 24$ (red dashed line), in agreement with the results in Ref. [30, 31].